SOLAR STRUCTURE INVERSION WITH LOWL DATA

Sarbani Basu
Teoretisk Astrofysik Center, Danmarks Grundforskningsfond,
Institut for Fysik og Astronomi, Aarhus Universitet, DK-8000 Aarhus C, Denmark; E-mail: basu@obs.aau.dk

Jørgen Christensen-Dalsgaard
Teoretisk Astrofysik Center, Danmarks Grundforskningsfond, and
Institut for Fysik og Astronomi, Aarhus Universitet, DK-8000 Aarhus C, Denmark; E-mail: jcd@obs.aau.dk

Jesper Schou
HEPL Annex A201, Stanford University, CA 94305-4085, USA; E-mail: schou@skaelv.stanford.edu

Michael J. Thompson
Astronomy Unit, School of Mathematical Sciences, Queen Mary and Westfield Colleges, Mile End Road,
London E1 4NS, UK; E-mail: M.J.Thompson@qmw.ac.uk

Steven Tomczyk
High Altitude Observatory, NCAR, P.O. Box 3000, Boulder, CO 80307, USA; E-mail: tomczyk@hao.ucar.edu

ABSTRACT

We present inversion results for the radial hydrostatic structure of the Sun, using six months of oscillation data obtained with the LOWL instrument. This is the first extensive homogeneous set of resolved data including both low- and intermediate-degree modes. We thus avoid systematic errors that might have been introduced into previous inversions by the merging of more than one data set. Using modes with degrees from 0 to 90 and frequencies between 1.5 and 3.5 mHz, we have inferred the variation with depth of the sound speed, density ρ and $u = p/\rho$ (p being pressure) from $r = 0.05R$ to $0.85R$. We find that in this region the sound speed in the Sun is within 0.15% of that of a model constructed using the MHD equation of state and OPAL opacities and incorporating helium diffusion. The density difference between Sun and model is less than 0.8%. Given the small error bars on our inversion results these small differences are significant, however. The solar sound speed appears to be higher than in the model for $r < 0.2R$. We speculate that this might indicate interesting physics in the inner core.

1. INTRODUCTION

Detailed observations of solar oscillations have provided us with accurate measurements of p-mode frequencies which impose severe constraints on the structure of the Sun. Inversion of solar frequencies available so far (e.g., Libbrecht et al. 1990; Elsworth et al. 1994; Bachmann et al. 1995) has revealed that current solar models differ from the Sun by only a few percent in sound speed and density (e.g., Däppen et al. 1991; Antia & Basu 1994; Dziembowski et al. 1994). These inversions suffer from one drawback, however: they were based on more than one set of data. Generally, frequencies of low-degree modes, with $0 \leq l \leq 3$, were obtained from full-disk observations, whereas higher-l modes were observed with spatial resolution. Such combinations of data may introduce systematic errors, either due to differing effects of magnetic activity in observations obtained at different epochs or because of different characteristics of the instruments and the data reduction procedures.

Here we present the initial results of inversion for the radial structure of the Sun using oscillation data obtained by the LOWL instrument. This is the first set of resolved data available for both low- and intermediate-degree modes. Since no combination of data is involved our results are free from the possible systematic errors mentioned above. We may therefore hope to obtain reliable estimates of the solar structure.

We have analyzed the frequencies to infer the sound-speed, density, and $u = p/\rho$ (ρ being density and p pressure) in the Sun. To put our results in context we also present results obtained from other data sets extensively used in previous inversions.

2. THE DATA

The data used for this work were obtained with the LOWL instrument (see Tomczyk et al. 1995). The instrument provides full disk images of the doppler shift of the solar potassium line at 769.9 nm with a spatial resolution of 25 arc sec at a cadence of one image per minute. It is located at an altitude of 3414 m on the Mauna Loa, Hawaii. The observations were made between February 26 and August 26, 1994, with a duty cycle of approximately 20 %. We use a total of 892 modes, illustrated in an $l - \nu$ diagram in Figure 1, with degrees from 0 to 90 in the frequency range 1.5 mHz to 3.5 mHz. To compare the results obtained from the LOWL frequencies with

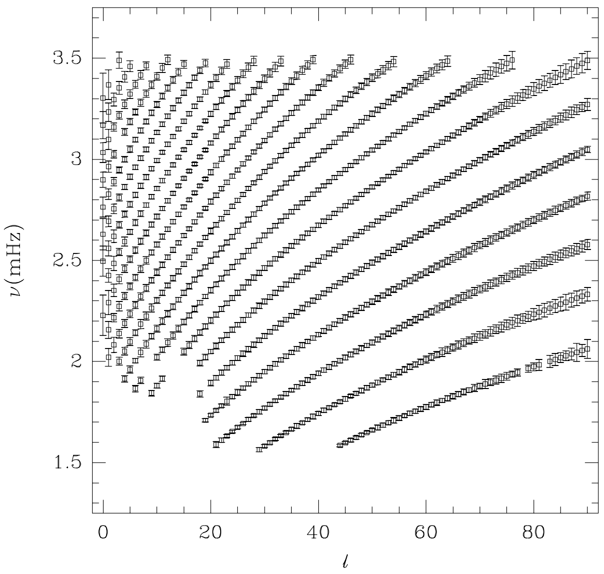

Figure 1. The $l-\nu$ diagram of the modes used in this work, indicated by $500\,\sigma$ error bars.

those available earlier, we have also inverted various combinations of modes involving the Big Bear Solar Observatory data for $l \geq 3$ as given by Libbrecht et al. (1990; in the following BBSO), BISON frequencies (Elsworth et al. 1994) for $l = 0-3$ and IPHIR frequencies (Toutain & Fröhlich 1991) for $l = 0-2$.

3. THE INVERSION TECHNIQUE

We assume that the oscillations can be described by linear adiabatic theory. By linearizing the differences in frequency and structure around a known solar model, the inverse problem can be written as

$$\frac{\delta\omega_i}{\omega_i} = \int K_i^{(1,2)}(r)\frac{\delta f_1(r)}{f_1(r)}\mathrm{d}\,r + \int K_i^{(2,1)}(r)\frac{\delta f_2(r)}{f_2(r)}\mathrm{d}\,r + \frac{F(\omega_i)}{\mathcal{E}_i}\,, \qquad (1)$$

where $\delta\omega_i$ is the difference in the frequency ω_i of the i^{th} mode between the solar data and a reference model. The functions f_1 and f_2 are an appropriate pair of model parameters. The kernels $K_i^{(1,2)}$ and $K_i^{(2,1)}$ are known functions of the reference model which relate the changes in frequency to the changes in f_1 and f_2 respectively. The term in $F(\omega)$ results from the near-surface errors in the physics of the reference model, including the assumption of adiabaticity, and the effect of surface boundary conditions in the frequency and kernel calculations. It may be argued that such effects give rise to a term of this form, with $F(\omega)$ being a slowly varying function of frequency and $\mathcal{E}_i$ is the inertia of the mode (cf. Christensen-Dalsgaard 1986; see also Rosenthal et al., these proceedings).

The pair (f_1, f_2) can involve several combinations of model parameters. In this work we use (c^2, ρ) to invert for c^2. To invert for ρ and u we use the pairs (ρ, Y), and (u, Y) respectively, where Y is the helium abundance. We note that the transformation to kernels involving Y requires the assumption that the equation of state and the heavy-element abundance are known.

We use the method of subtractive optimally localised averages (henceforth SOLA; cf. Pijpers & Thompson 1994; Christensen-Dalsgaard & Thompson 1995), to carry out the inversions. Thus we choose coefficients $c_i(r_0)$ in such a way that the linear combination

$$\mathcal{K}_{1,2}(r_0, r) = \sum_i c_i(r_0) K_i^{(1,2)}(r) \qquad (2)$$

is a well-localised averaging kernel at target radius r_0. In the SOLA technique this is achieved by minimizing the difference between $\mathcal{K}_{1,2}(r_0, r)$ and a target kernel $\mathcal{T}(r_0, r)$. We have used target kernels of Gaussian shape. The minimization is carried out subject to the condition that the sum

$$\mathcal{C}_{1,2}(r_0, r) = \sum_i c_i(r_0) K_i^{(2,1)}(r) \qquad (3)$$

and the error in the corresponding combination of the data are small (for details, see Christensen-Dalsgaard & Thompson 1995). In this case the sum

$$\left(\frac{\delta f_1}{f_1}\right)_{\mathrm{inv}} = \sum_i c_i \frac{\delta\omega_i}{\omega_i} \qquad (4)$$

provides a well-localised average of the first function $\delta f_1/f_1$.

The surface term $F(\omega)$ is taken care of by constraining the solution to remain unchanged in the presence of slowly varying functions of frequency in the data. This is done by adding constraints of the form

$$\sum_i c_i(r_0)\mathcal{E}_i^{-1} P_\lambda(x_i) = 0\,, \quad \lambda = 0, \ldots, \Lambda\,, \qquad (5)$$

where

$$x_i = \frac{\max(\omega_i) + \min(\omega_i) - 2\omega_i}{\max(\omega_i) - \min(\omega_i)}\,, \qquad (6)$$

and P_λ is the Legendre polynomial of degree λ. We choose $\Lambda = 10$.

4. THE REFERENCE MODEL

With the exception of the equation of state, the reference model corresponds essentially to Model 2 of Christensen-Dalsgaard, Proffitt & Thompson (1993). It was constructed with the MHD equation of state (Hummer & Mihalas 1988; Mihalas, Däppen & Hummer 1988; Däppen et al. 1988), OPAL opacities (Iglesias, Rogers & Wilson 1992) in the high temperature regions and Kurucz (1991) opacities in the atmosphere. The heavy-element abundance was $Z = 0.02$.

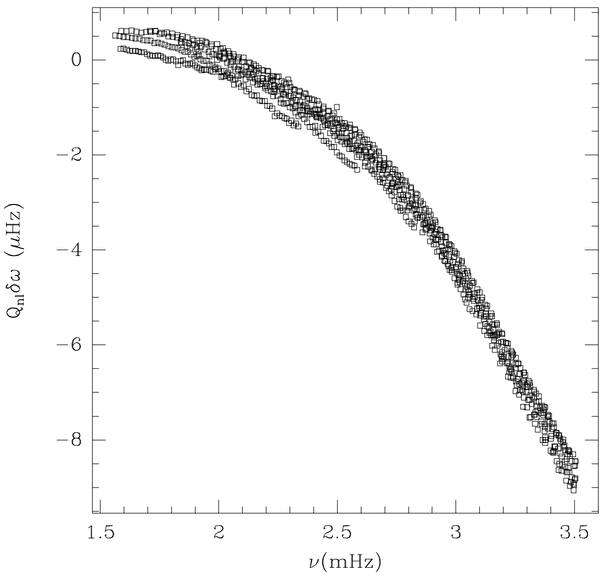

Figure 2. Frequency differences between the LOWL data set and the reference model used in this work, in the sense (Sun) – (model). The differences have been scaled by the ratio Q_{nl} between the mode inertia and the inertia of a radial mode of the same frequency

The model incorporates diffusion of helium below the convection zone. It was calibrated to have solar photospheric radius ($\mathrm{R}_\odot = 6.9599 \times 10^{10}\,\mathrm{cm}$) and solar luminosity ($3.846 \times 10^{33}\,\mathrm{erg\,s^{-1}}$) at an age of 4.6×10^9 years, resulting in initial and present surface helium abundances of $Y_0 = 0.276$ and $Y_\mathrm{s} = 0.248$, respectively. The base of the convection zone is at a radius of $0.706\,\mathrm{R}_\odot$, and the central temperature, density and pressure of the model are $15.66 \times 10^6\,\mathrm{K}$, $154\,\mathrm{g\,cm^{-3}}$ and $2.33 \times 10^{17}\,\mathrm{dyne\,cm^{-2}}$, respectively.

Figure 2 shows differences between the observed frequencies from the LOWL data and the frequencies of this model, scaled by the normalized mode inertia. It is evident that the differences are dominated by the term in $F(\omega_i)$ (cf. equation 1), although small departures from this trend, associated with differences in the interior, are also visible.

4. RESULTS FOR THE LOWL DATA

The results of the inversions for sound-speed, density and u are shown in Figs 3, 4 and 5 respectively. In each figure the vertical error bars are the errors in the solution obtained from the quoted observational errors in the data, while the horizontal error bars are measures of the resolution of the inversion, defined as the distance between the quartile points of the averaging kernels.

The sound-speed inversion does not involve any additional assumptions about the physics of the solar interior; thus we believe that it is the most robust. In contrast, the density and u inversions, which use

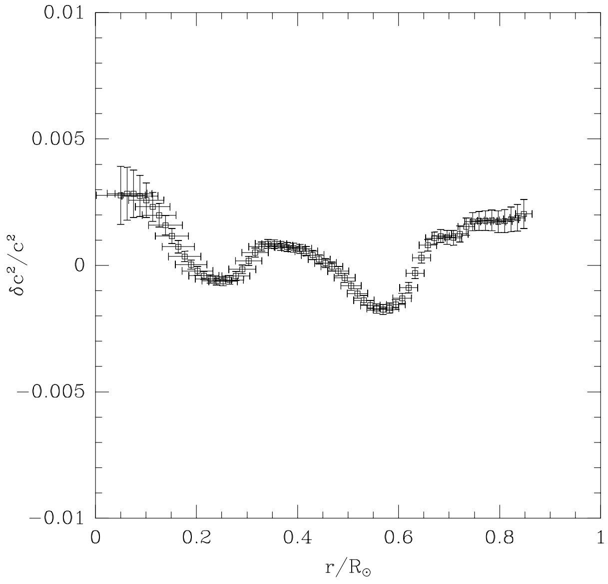

Figure 3. The inferred difference in the squared sound speed, in the sense (Sun) – (model), obtained from inversion of the LOWL data

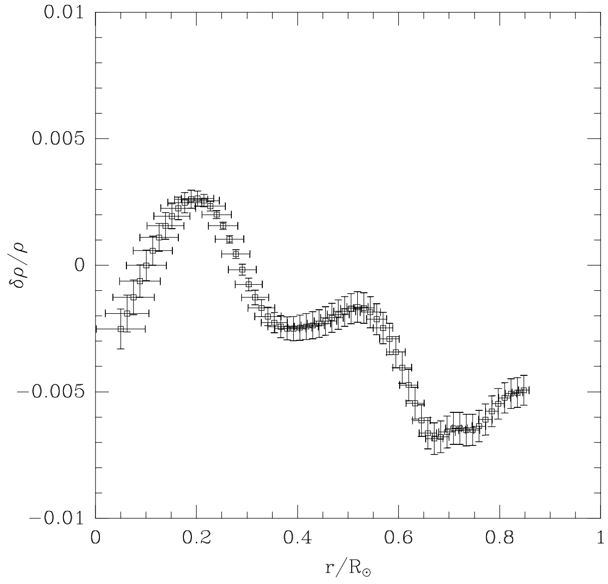

Figure 4. The inferred difference in density, obtained from inversion of the LOWL data

Y as the second variable, assume that the equation of state of the solar material is known. This introduces some uncertainty in the results. We note, however, that Pérez Hernández & Christensen-Dalsgaard (1994) found indications that the MHD equation of state is a good approximation to the properties of the solar matter in the helium ionization zone, lending some confidence to our results for ρ and u. This is supported by the near agreement between the results for u and c^2 in the deep interior, where Γ_1 would be expected to be almost constant.

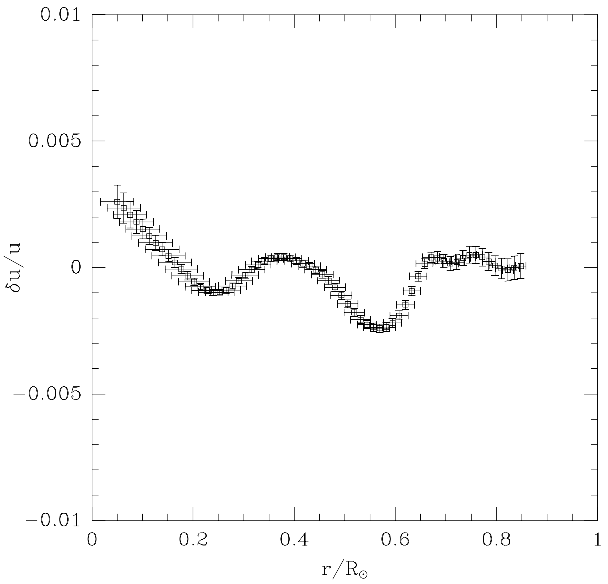

Figure 5. The inferred difference in $u = p/\rho$, obtained from inversion of the LOWL data

The figures show that the hydrostatic structure of the Sun is very similar to that of the reference model. The sound speed of the model is within 0.15% of that of the Sun, while density is correct to within 0.8%. However, given the very small error bars, the differences are clearly significant. From the results on sound speed and u it follows that the base of the convection zone is deeper in the model than in the Sun. This result is consistent with earlier estimates which gave the position of the base of the solar convection zone as $0.713\,\mathrm{R}_\odot$ (Christensen-Dalsgaard et al. 1991). An interesting feature is the rise in the solar sound speed, and decrease in the density, relative to the model at the centre. This could indicate that some partial mixing has occured in the inner core; another possibility is that the opacities there need modification (Basu et al. 1995, in preparation).

5. COMPARISON WITH RESULTS FOR OTHER OBSERVATIONS

To compare our inversion results with those obtained previously we have inverted various other sets of data. As mentioned earlier, no other set of frequencies covers the range in degree from 0 to reasonably high values. Hence it is necessary to combine data sets. We have inverted several different combinations of the BBSO, BISON and IPHIR data, as well as combinations of the latter two sets with LOWL data. These combinations are summarized in Table 1.

The results of the sound-speed inversions for the sets B1, B2 and I1 are shown in Figs 6 and 7. In the bulk of the solar interior, the sound-speed differences are very similar. In particular, the combinations B1 and I1 give almost identical results in the range $0.25 \le r \le 0.85\,\mathrm{R}_\odot$. This is not surprising since the identical high-l frequencies were used in both cases. However, the results for the set B2, where the frequency range for the BBSO modes is restricted to be the same as for the LOWL data, deviate significantly from B1 and I1 in the dip around $0.25\,\mathrm{R}_\odot$, while being close to the results from the LOWL data in this region. This indicates that the high-frequency modes in sets B1 and I1, which are not present in B2, are responsible for the feature.

Table 1. Different data combinations used

	Low ℓ set	Intermediate ℓ set
B1	BISON $0 \le \ell \le 3$	BBSO $4 \le \ell \le 100$ $(1.0 \le \nu \le 5$ mHz)
B2	BISON $0 \le \ell \le 3$	BBSO $4 \le \ell \le 100$ $(1.0 \le \nu \le 3.5$ mHz)
B3	BISON $0 \le \ell \le 3$	LOWL $4 \le \ell \le 90$
I1	IPHIR $0 \le \ell \le 2$	BBSO $4 \le \ell \le 100$ $(1.0 \le \nu \le 5$ mHz)
I2	IPHIR $0 \le \ell \le 2$	LOWL $3 \le \ell \le 90$

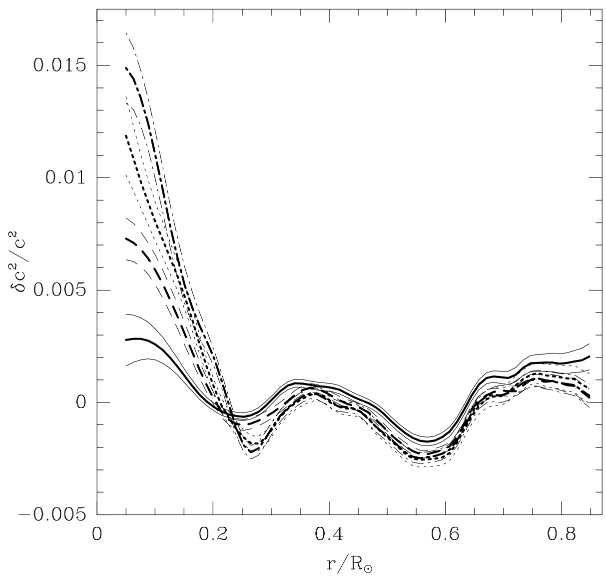

Figure 6. A comparison of results of sound-speed inversions obtained from different sets of solar data. The thick lines are the results while the thin lines give 1σ error bounds. The continuous line is the results obtained by the LOWL data. The dotted line is that obtained using the combination B1 of BISON and BBSO data, while the dashed line is for the combination B2. The dot-dashed line is the inversion result for mode set I1

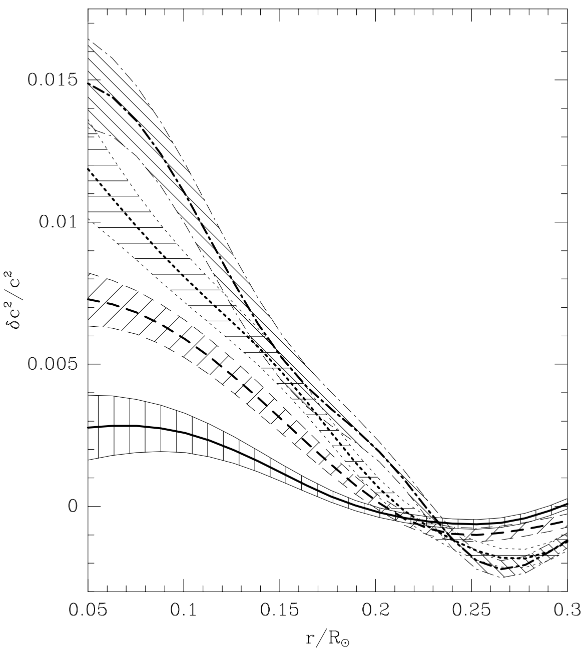

Figure 7. A blow-up of the region $r \leq 0.3\,\mathrm{R}_\odot$ in Fig. 6. The line types are the same as in Fig. 6, but in addition for clarity we have shaded the 1σ bounds of the various results. The region with vertical shading was obtained by inversion of the LOWL data, horizontal shading is the region obtained from the set B1, the sparse slanted shading is for set B2 and the dense slanted shading is for I1

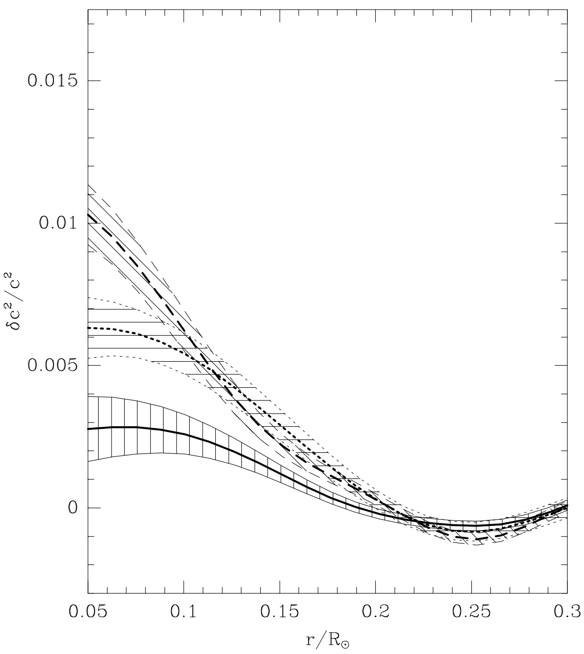

Figure 8. The sound-speed inversion results of the LOWL data (continuos line, vertical shading), the combination B3 (dotted line, horizontal shading), and the combination I2 (dashed line, slanted shading)

We note that the same widths of the averaging kernels, as functions of target position, were used for the inversion of all sets of data. Thus the effect of including high-frequency modes does not arise from an increase in resolution, but is probably a result of systematic errors in the data.

The most striking difference is in the solar core, however. This is seen most clearly in the blow-up of the central region in Fig. 7. The combination I1 yields the highest value of sound speed in this region. Using B1 results in a slightly lower value, while LOWL shows the best agreement between the Sun and the model. The results obtained with B2 are very interesting. Since the low-l modes, which give information about the centre, are identical for B1 and B2 it could be expected that the inversion results should be similar. However, we find that the results of B2 are more than 2σ lower than those of B1. This clearly indicates the importance of the higher-l modes for inversions in the solar core.

To check this further we have inverted the combinations B3 and I2 of the BISON and IPHIR modes with the LOWL modes at higher degree. The results are shown in Fig. 8. A comparison with Fig. 7 shows that the use of LOWL instead of BBSO with the BISON and IPHIR low-l modes lowers the sound-speed difference between the Sun and the model in the core, once again indicating the sensitivity of the results to the choice of high-degree modes. It is evident that great care is required when matching the the intrinsically very accurate low-degree data from the whole-disk instruments with higher-degree data for the purpose of carrying out inversions.

6. CONCLUSIONS

We have inverted solar oscillation frequencies obtained by the LOWL instrument to infer the radial hydrostatic structure of the Sun, as described by differences in the sound speed, density, and $u = p/\rho$ between the Sun and a solar model. The sound speed of the model is within 0.15% of that in the Sun, while the relative difference in density is less than 0.8%.

The sound speed in the region $r < 0.2\,\mathrm{R}_\odot$ appears to be higher than in the model, indicating potentially interesting physics in the inner core. However, the sound speed in the core inferred from the LOWL data is closer to the model than that obtained from either the IPHIR or the BISON data. The results for the latter two low-degree sets depend strongly on the choice of higher-degree modes used, the variation exceeding substantially the inferred uncertainty due to the random data errors. This emphasizes the value of carrying out inversion on homogeneous sets of data, such as the LOWL set.

ACKNOWLEDGMENTS

This work was supported by the Danish National Research Foundation through its establishment of the Theoretical Astrophysics Center, the National Aeronautics and Space Administration through grant NAS5-30386, the US National Science Foundation through base funding of HAO/NCAR, and the UK Particle Physics and Astronomy Research Council under grant no. GR/J00588.

REFERENCES

Antia H. M., Basu S., 1994b, A&AS, 107, 421

Bachmann K. T., Duvall T. L., Jr., Harvey J. W., Hill F. 1995, ApJ, 443, in press

Christensen-Dalsgaard J., 1986, in: Seismology of the Sun and the distant Stars, ed. Gough D. O., Reidel, Dordrecht, p. 23

Christensen-Dalsgaard J., Thompson M. J., 1995, in: Ulrich, R. K., Rhodes Jr, E. J., Däppen, W., eds, Proc. GONG'94: Helio- and Astero-seismology from Earth and Space, PASPC vol. 76, 144

Christensen-Dalsgaard J., Gough D. O., Thompson M. J. 1991, ApJ, 378, 413.

Christensen-Dalsgaard J., Proffitt C. R., Thompson M. J., 1993, ApJ, 403, L75

Däppen W., Gough D. O., Kosovichev A. G., Thompson M. J., 1991, in: Challenges to theories of the structure of moderate-mass stars, Lecture Notes in Physics, vol. 388, eds Gough, D. O., Toomre, J., Springer, Heidelberg, p. 111

Däppen W., Mihalas D., Hummer D. G., Mihalas B. W., 1988, ApJ, 332, 261

Dziembowski W. A., Goode P. R., Pamyatnykh A. A., Sienkiewicz R., 1994, ApJ, 432, 417

Elsworth Y., Howe R., Isaak G.R., McLeod C.P., Miller B.A., New R., Speake, C. C., Wheeler S.J. 1994, ApJ, 434, 801

Hummer D. G., Mihalas D., 1988, ApJ, 331, 794

Iglesias C. A., Rogers F. J., Wilson B. G., 1992, ApJ, 397, 717

Kurucz R. L., 1991, in: Stellar atmospheres: beyond classical models, eds Crivellari L., Hubeny I., Hummer D. G., NATO ASI Series, Kluwer, Dordrecht, p. 441

Libbrecht K. G., Woodard M. F., Kaufman J. M. 1990, ApJS, 74, 1129.

Mihalas D., Däppen W., Hummer D. G., 1988, ApJ, 331, 815

Pérez Hernández F., Christensen-Dalsgaard J., 1994, MNRAS, 475

Pijpers F. P., Thompson M. J., 1994, A&A, 281, 231

Tomczyk S., Streander K., Card G., Elmore D., Hull H., Cacciani A., 1995, Sol. Phys., in press

Toutain T., Fröhlich C. 1991, A&A 257, 287